Journal Pre-proofs

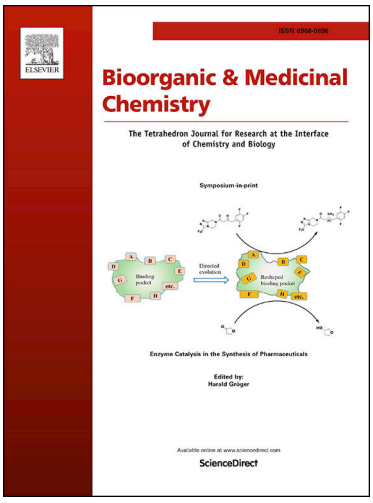

In Situ Localization of Alkaline Phosphatase Activity in Tumor Cells by an Aggregation-Induced Emission Fluorophore-Based Probes

Qinghua Guan, Xinmiao Lu, Yue Su, Jichen Xu, Xiaofei Liang, Peiyong Li, Xinyuan Zhu

PII: S0968-0896(19)31530-5
DOI: https://doi.org/10.1016/j.bmc.2019.115284
Reference: BMC 115284

To appear in: *Bioorganic & Medicinal Chemistry*

Received Date: 10 September 2019
Revised Date: 13 December 2019
Accepted Date: 18 December 2019

Please cite this article as: Q. Guan, X. Lu, Y. Su, J. Xu, X. Liang, P. Li, X. Zhu, In Situ Localization of Alkaline Phosphatase Activity in Tumor Cells by an Aggregation-Induced Emission Fluorophore-Based Probes, *Bioorganic & Medicinal Chemistry* (2019), doi: https://doi.org/10.1016/j.bmc.2019.115284

This is a PDF file of an article that has undergone enhancements after acceptance, such as the addition of a cover page and metadata, and formatting for readability, but it is not yet the definitive version of record. This version will undergo additional copyediting, typesetting and review before it is published in its final form, but we are providing this version to give early visibility of the article. Please note that, during the production process, errors may be discovered which could affect the content, and all legal disclaimers that apply to the journal pertain.

© 2019 Published by Elsevier Ltd.

In Situ Localization of Alkaline Phosphatase Activity in Tumor Cells by an Aggregation-Induced Emission Fluorophore-Based Probes

Qinghua Guan,[1,2,†] Xinmiao Lu,[1,2†] Yue Su,[2] Jichen Xu,[3] Xiaofei Liang,[3] Peiyong Li,*[,1] Xinyuan Zhu*[,2]

1 Department of Nuclear Medicine, Ruijin Hospital, School of Medicine, Shanghai Jiao Tong University, Shanghai 200025, China

2 School of Chemistry and Chemical Engineering, State Key Laboratory of Metal Matrix Composites, Shanghai Jiao Tong University, 800 Dongchuan Road, Shanghai 200240, China

3 State Key Laboratory of Oncogenes and Related Genes, Shanghai Cancer Institute, Renji Hospital, School of medicine, Shanghai Jiaotong University, No. 25/Ln 2200 Xie Tu road, Shanghai 200032, China

† Authors who made equal contribution in this work and were considered as co-first authors.

Correspondence author: Peiyong Li, Department of Nuclear Medicine, Ruijin Hospital, School of Medicine, Shanghai Jiao Tong University, Shanghai 200025, P. R. China. Tel: + 86-21-34188822, fax: + 86-21-34188822, Email: peiyli@vip.sina.com

Correspondence author: Xinyuan Zhu, School of Chemistry and Chemical Engineer, Shanghai 200240, P. R. China. Tel: + 86-21-34206899, fax: + 86-21-54741297, Email: xyzhu@sjtu.edu.cn

Journal Pre-proofs

ABSTRACT

In situ detection of certain specific enzyme activities in cells is deeply attached to tumor diagnosis. Conventional enzyme-responsive fluorescent probes have difficulty detecting targeted enzymes in situ in cells due to the low detection accuracy caused by the spread of fluorescence probes. In order to solve this problem, we have designed and synthesized an enzyme-responsive, water-soluble fluorescent probe with AIE characteristics, which could aggregate and precipitate to produce in situ fluorescence when reacting with the targeted enzyme in cells. The AIE fluorophore (TPEQH) was utilized to design the enzyme-responsive, fluorescent probe (TPEQHA) by introducing a phosphate group on to it, which could be specifically decomposed by the targeted enzyme, namely alkaline phosphatase (ALP). In tumor cells, TPEQH was highly produced due to the interaction of phosphate on the TPEQHA and the overexpressed ALP. Water-insoluble TPEQH then precipitated and release fluorescence *in situ*, thereby successfully detecting the ALP. Furthermore, the expression level of ALP could be determined by the fluorescence intensity of TPEQH with higher accuracy due to the inhibition of TPEQH leak, which demonstrated a potential application of in suit ALP detection in both clinical diagnosis and scientific research of tumor.

KEYWORDS: AIE probe, ALP, tumor fluorescence imaging

1. INTRODUCTION

Fluorescent probes have been deemed as powerful tools for optical imaging and analysis due to its ability to directly visualize the biological analytes at molecular level and provide delicate information of complex biological structures and processes[1-9]. However, current fluorescent probes are generally based on the aggregation-caused quenching (ACQ) fluorophores, which need

design as cytoplasm soluble probes in living cell imaging, such as specific imaging for a certain enzyme.[10,11] Therefore, the responsive products of ACQ probes and targeted enzyme easily diffuse away from the original generation site, leading to the unsatisfied resolution and contrast of images.[12-14] Hence, it is imperative to develop fluorescent probes, which have capacity of conducting high-resolution and in situ imaging and improve the imaging contrast and accuracy of the detection results.

To address these limitations, a well-established method is to design a fluorescent probe, which can generate insoluble fluorescent products after specific respond with target and gather in situ to emit fluorescence. Unfortunately, ACQ fluorophores have intrinsic difficulty meeting this requirement due to the quenched fluorescence after aggregation.[15] However, with the development of new aggregation-induced emission (AIE) fluorophores, which show exactly opposite natures to the ACQ fluorophores, this dilemma is expected to be resolved.[16,17] AIE fluorophores are a series of fluorescence molecules showing faint or quenched fluorescence in the dilute solutions but bright and obvious fluorescence in the state of aggregation. Obviously, this unique photophysical phenomenon makes it an ideal precursor to design in situ fluorescent probes.

In this context, an AIE fluorescent probe to detect targeted alkaline phosphatase (ALP) in living cells was designed based on a new AIE fluorophore TPEQH (Scheme 1). TPEQH is a typical AIE fluorophore, which is hydrophobic and emits bright fluorescence in the state of aggregation or solid state. Apart from that, TPEQH had long excitation wavelength and large Stokes Shift, which contributed to high sensitivity, low background signal and high non-target contrast during imaging.[18-21] Additionally, its hydrophilicity and water solubility could be easily regulated by modifying the hydroxyl group on the TPEQH. Meanwhile, ALP is a crucial biomarker for tumor diagnosis in clinical because the expression level of ALP in peripheral blood is significantly

increased in many cancer patients. Thence, TPEQH was utilized to design an ALP-responsive, fluorogenic probe (TPEQHA) by modifying a phosphate group onto the phenolic hydroxyl group of TPEQH. ALP is a kind of hydrolase which are capable of hydrolyzing phosphate bond on lots of substrates.[22-28] Therefore, when phosphate bond of TPEQHA was specifically decomposed by ALP, free TPEQH was released and precipitated in a very short time. The solid-state fluorescence molecule could emit bright fluorescence and successfully detected and imaging ALP in living cells with high resolution and accuracy.

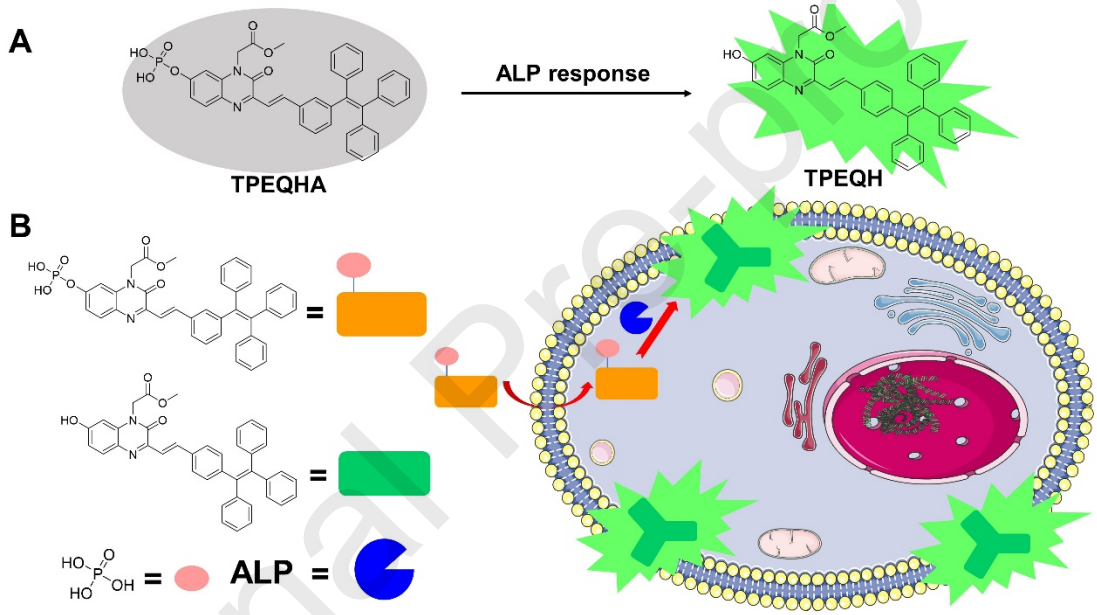

Scheme 1. In-situ fluorescence imaging of tumor cells with TPEQHA [a]

[a](A) Imaging of TPEQHA in Tumor Cell. (A) The water-soluble TPEQHA was hydrolyzed by ALP to become a liposoluble TPEQH, which was aggregated in an aqueous solution to induce fluorescence. (B) In tumor cells, TPEQHA was hydrolyzed by ALP on cytomembrane and aggregated to induce fluorescence.

2. EXPERIMENTAL SECTION

Journal Pre-proofs

2.1 Materials. Benzene-1,2-diamine, ethyl-2-oxopropanoate and methyl-2-bromoacetate were bought from Tokyo Chemical Industry Co., Ltd. 4-(1,2,2-triphenylethenyl)benzaldehyde, boron tribromide and phosphorus oxychloride were purchased from J&K Scientific Ltd. 4-(1,2,2-Triphenylethenyl)benzaldehyde was acquired (TPE-CHO) from Zhengzhou Alfachem Co., Ltd. Tetrahydrofuran (THF), K_2CO_3, ethyl acetate, *N,N*-dimethylformamide (DMF) and dichloromethane (DCM) were bought from Adamas.

2.2 Synthesis of 7-Methoxy-3-methylquinoxalin-2(1H)-one (1). To obtained molecule 1, benzene-1,2-diamine (13.8 g) and anhydrous ethanol (150 mL) were added into a beaker and the temperature was lowered to 0 ℃. After that, ethyl pyruvate (13.92 g) dissolving in ethanol (10 mL) was added dropwise. After gradually returning to 25 ℃, the mixture kept reacting for 10 h under magnetic stirring. During the reaction, the insoluble solid product gradually precipitated in the solution. After the reaction, the product was then filtered and washed with anhydrous ethanol, followed by the removal of ethanol in vacuum, 16.53 g white solid was obtained in 87% yield. ^{1}H-NMR and MS spectroscopy were used to identify the product, Figure S1. [LC-MS] m/z: 191.0804 $[M+H]^+$.

2.3 Synthesis of Methyl-2-(7-methoxy-3-methyl-2-oxoquinoxalin-1(2H)-yl)acetate (2). To synthesize compound (2), into the acetone were suspended with 3.8 g compound (1) and 3.67 g methyl-2-bromoacetate, followed by the treatment of vigorous stirring. After that, 3.31 g K_2CO_3 was added, the mixture kept reacting under reflux at 62 ℃ for 12 h. After reaction, the the solid residues were filtered and the solution was treated with rotary evaporators to remove the acetone. The solute was then redissolved in ethyl acetate (EA, 50 mL) again and washed by deionized water for 3 times. After washing, the organic phase was dried with anhydrous $MgSO_4$, followed by the filtration to remove $MgSO_4$. The solvent was then removed in vacuum to obtain the white crude

product. The product was then purified by recrystallization in EA/PE, and 2.72 g product was obtained in 52% yield. ^{1}H-NMR and MS spectra were used to confirm the successful synthesis, shown in Figure S2. [LC-MS] m/z: 263.1021 $[M+H]^+$.

2.4 Synthesis of Methyl-2-(7-hydroxy-3-methyl-2-oxoquinoxalin-1(2H)-yl)acetate (3). Eggplant bottle containing compound (2) (524 mg) was evacuated and filled with nitrogen.10 mL DCM was added and the solution was cooled to -25 ℃. Then, BBr_3/CH_2Cl_2 solution (1 M) was added dropwise and the mixture gradually turned bright red. After returning to room temperature, the mixture continued to react for 24 hours. The reaction was then quenched by adding 10 mL H_2O after the solution was cooled to 0 ℃ again. The solution was adjusted to pH 8 with NH_3 solution (5 M) and the water phase was separated in a separatory funnel. The water phase was washed with DCM (10 mL × 3) and adjusted to pH 3 with $KHSO_4$ solution (2 M) to induce the precipitation of solid product. After filtration, the solid was dried in vacuum and light yellow production was obtained after purification using silica chromatography (dichloromethane : methanol = 30:1) (213 mg, 43%). The product was characterized by ^{1}H-NMR and MS, Figure S3. [LC-MS] m/z: 249.0867 $[M+H]^+$.

2.5 Synthesis of Methyl(*E*)-2-(7-hydroxy-2-oxo-3-(4-(1,2,2-triphenylvinyl)styryl)-quinoxalin-1(2H)-yl)acetate (4, TPEQH). Compound (3) (496 mg) were added into the flask containing 10 mL acetic acid under magnetic stirring, followed by the addition of 4-(1,2,2-triphenylethenyl) benzaldehyde (FTPE, 1.08 g) to obtained the suspension. After that, 100 μL catalytic amount of concentrated H_2SO_4 was carefully dripped into the suspension and the mixture kept reacting at 60 ℃ for 12 h. After reaction, the solution was cooled to room temperature and the mixture was dissolved with 60 mL DCM. The DCM solution was then washed with deionized water (15 mL × 3) and dried over anhydrous $MgSO_4$, followed by filtration to remove the $MgSO_4$.

The solvent wasthen removed in vacuum and solid product were obtained after pretreatment, which was further purified by silica chromatography (EA : PE = 1 : 4) to obtain pure yellow product (932 mg, 79% yield). The ^{1}H-NMR and MS spectra of final product were shown in Figure S4. [LC-MS] m/z: 591.2280 $[M+H]^+$.

2.6 Synthesis of Methyl(*E*)-2-(2-oxo-7-(phosphonooxy)-3-(3-(1,2,2-triphenylvinyl)styryl)-quinoxalin-1(2H)-yl)acetate (5, TPEQHA). TPEQH (295 mg) was suspended in dry DCM (50 mL) and treated with magnetic stirring at 0 ℃ in the nitrogen atmosphere. POCl3 (0.2 mL) and dry pyridine (0.3 mL) were added by syringe. The mixture then slowly returned to room temperature and reacted for 1 h. After reaction finished, ice water (50 mL) was added, and the reaction solution was extracted with CH_2Cl_2/EtOH. The combined organic phase was dried with Na_2SO_4 and concentrated under reduced pressure. After purified by silica gel chromatography (CH_2Cl_2/EtOH, 3:1, v/v), compound HTPQA was obtained as a colorless solid (134 mg, 40%). The NMR and MS spectra of the finical product were shown in Figure S5. [LC-MS] m/z: 688.19999 $[M+NH_4]^+$。

2.7 Spectra Characterization of the TPEQH. For the characterization of the TPEQH, the UV-Vis and photoluminescence spectra were applied to determine the spectra of TPEQH. Firstly, the excitation and emission wavelength of solid TPEQH were determined. Secondly, TPEOH was dissolved in THF to investigate both UV-Vis spectrum and excitation/emission spectra in solution (1×10^{-5} M). Furthermore, for investigating the emission spectrum in different polar solvents, TPEQH was dissolved in acetone, THF, DMSO and MeOH (1×10^{-3} M), and measured the fluorescence spectra.

2.8 Researches on the AIE performance of TPEQH. The AIE performance of TPEQH was then studied in the mixture solvent of THF and H_2O. Namely, the TPEQH solution (dissolved in

THF, 2×10^{-4} M, 100 μL) was mixed with different volume of pure THF (1900, 1700, 1300, 900, 500, 300, 100, 0 μL), followed by the addition of different volume of deionized water to adjusted the total volume to 2 mL (1×10^{-5} M). Additionally, the AIE performance of TPEQH in pure THF with different concentrations (1×10^{-2}, 1×10^{-3}, 1×10^{-4}, 1×10^{-5}, 1×10^{-6}, 1×10^{-7} M) was also determined. The excitation wavelength was set at 300 nm 353 nm.

2.9 Theoretical Investigations. Density functional theory (DFT) calculation was then applied to deep understand the AIE performance of TPEQH. The calculation was conducted with the Gaussian09 program.[29] Geometry optimization of TPEQH structure was calculated at B3LYP/6-31G* without any symmetry restriction.[30-32] After that, at the same level, analytical vibration frequencies were performed to determine the nature of the located stationary point.

2.10 The Fluorescence Response of TPEQHA to ALP. The fluorescence response of TPEQHA to ALP was studied using TPEQHA (100 μM) dissolved in DMSO and ALP solutions with different concentrations (0, 4, 10, 20, 40, 80, 120, 160, 200, 240, 320, 360 U/L in Tris-HCl solution). Namely, 100 μL of TPEQHA solution was diluted with 1900 μL Tris-HCl solution. In the TPEQHA solution (1 mL) was added into a series of ALP solution and incubated for 20 minutes at 37 ℃. The fluorescence spectra after response was then determined at the excitation wavelength of 465 nm.

2.11 In Vitro Cytotoxicity Study. HeLa and L929 cells were seeded in 96-well plates and incubated at 37 ℃ for 12 h. Then cells were treated with TPEQH at the concentration ranging from 0 to 20 μg/mL. After 2 d incubation, MTT solution was added into each well and incubated with cells for another 4 h. After incubation, the medium was carefully removed, and 200 μL DMSO was added into each well. After the addition of DMSO, plates were slightly shaken for 15 min.

Journal Pre-proofs

Finally, the DMSO solution was taken out and the absorbance of solution was determined at the wavelength of 570 nm.

2.12 Intracellular Imaging of TPEQHA. To further study the intracellular ALP response and fluorescence imaging of TPEQHA, ALP was detected in HeLa cells and L929 cells, which were considered as ALP positive cell and ALP negative control group respectively, using a confocal laser scanning microscopy (CLSM) and a flow cytometry. Furthermore, in order to determine the specificity of TPEQHA for ALP, HeLa cells treated with levamisole hydrochloride (1×10^{-3} M) was detected as positive control group.[33,34]

For the flow cytometry analysis, there types of cell samples (Hela cell, HeLa cell treated with levamisole hydrochloride and L929 cell) were seeded in 6-well plates at the density of 5×10^5 per well. After replacing the old medium with fresh medium containing TPEQHA (10 μM), cells were incubated for another 1 h. After incubation, medium was removed and cells were washed with fresh PBS for 3 times. Finally, cells were treated with trypsin and the digested cells were measured using a flow cytometer.

For the CLSM experiments, cells (3×10^5) were planted in the confocal dishes and cultured for 12 h in culture medium. After incubation, the original medium was removed and fresh medium containing TPEQHA (10 μM) was added. After incubating for another 1 h, medium was removed and cells were washed with fresh PBS. After washing, 1 mL PBS was added and the dishes were applied for CLSM imaging at a 488 nm laser. Apart from that, TPEQHA was replaced with 4-Methylumbelliferyl Phosphate (4-MUP) and observed at a 405 nm laser.

2.13 Statistical Analysis. The results are illustrated as the mean ± standard deviation (SD). The difference was evaluated by Student's *t* test, and considered statistically significant if $p < 0.05$ (*), respectively.

Journal Pre-proofs

3. RESULTS AND DISCUSSION

3.1 Preparation and Characterization of TPEQH and TPEQHA. The synthetic processes of TPEQH and TPEQHA were shown in Figure 1. The TPEQH was obtained by the Aldol Reaction of 4-(1,2,2-triphenylethenyl)benzaldehyde and methoxy quinoxalinone (MQX), while MQX was synthesized according to the method we previously reported.[48] TPEQHA was then prepared based on TPEQH to stnthesize AIE fluorescent probe. The ^{1}H-NMR, ^{13}C-NMR and LC-MS were used to prove the successful synthesis in each step (Figure S1-S6).

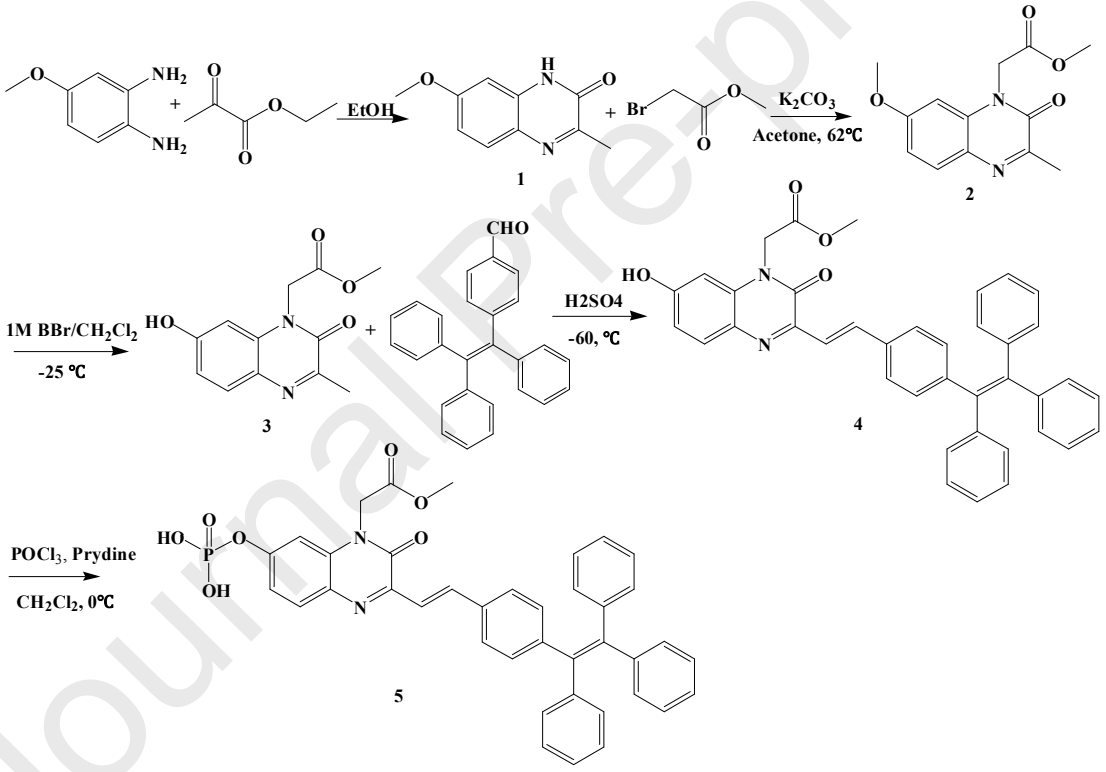

Figure 1. Synthesis of TPEQH and TPEQHA.

After the synthesis of TPEQH, its photophysical properties including UV-vis absorption and fluorescent spectra were investigated. As shown in Figure 2A, TPEQH presented with wide excitation wavelength (ranged from 350 – 510 nm) and its maximum emission wavelength was

Journal Pre-proofs

located at 663 nm. These results meant that TPEQH not only had excellent AIE property, but also had a large Stokes shift. Moreover, UV-vis absorption spectrum in THF solution was shown in Figure 2B, indicating that TPEQH exhibited strong UV-vis absorption from 350 nm to 450 nm, which might be attributed to the π-π* transition of the TPEQH.

Finally, the solvatochromic properties of TPEQH were detected in organic solutions of different polarities (THF < Acetone < DMSO < MeOH). The UV-Vis absorption and fluorescent emission spectra were shown in Figure 2C and 2D. The UV-Vis absorption spectra were almost similar in different solutions. However, with the solvent polarity increasing, a red shift was observed in the emission spectrum, which might result from the intramolecular charge-transfer of TPEQH.[49-54]

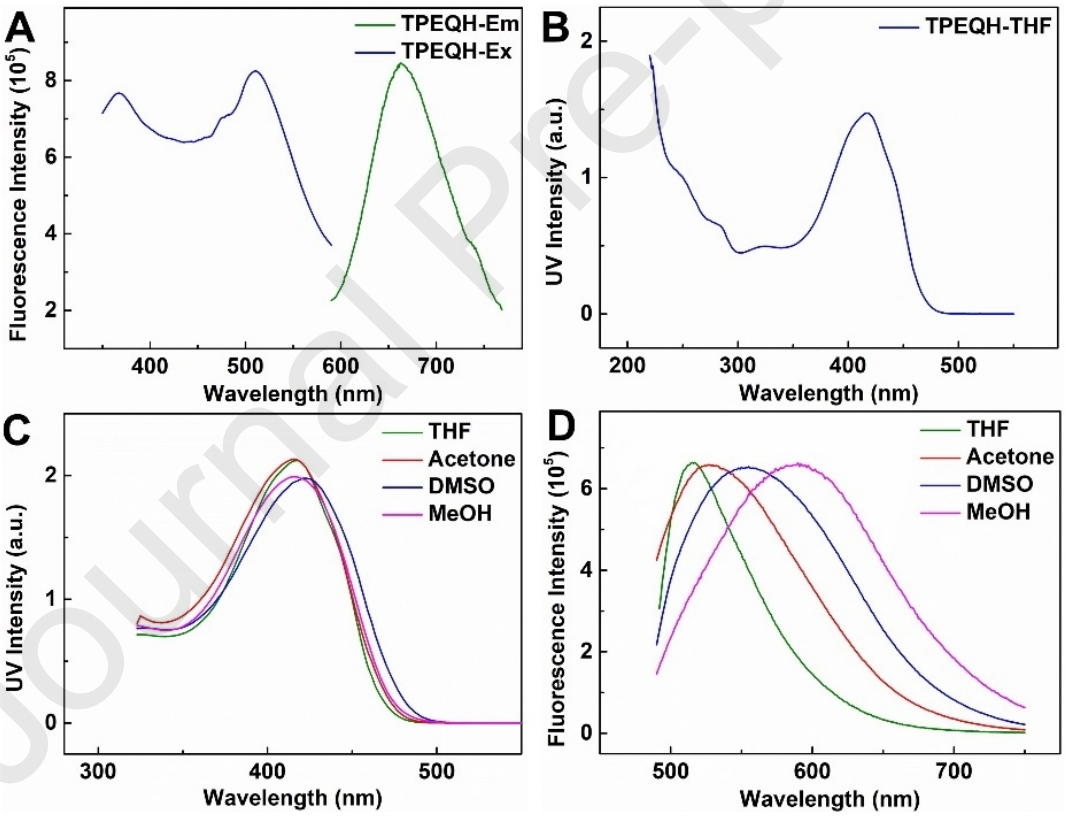

Figure 2. Optical properties of TPEQH. (A) Fluorescent excitation and emission spectra of TPEQ solid. (B) The UV-vis absorption spectrum of TPEQ in pure THF (1×10^{-5} M). (C) The UV-Vis absorption spectrum of TPEQ (1×10^{-5} M) in different solution (THF, Acetone, DMSO,

MeOH). (D) The fluorescent emission spectra of TPEQ (1×10^{-3} M) in different solution (THF, Acetone, DMSO, MeOH) with 475 nm laser.

3.2 AIE Property. To obtain the insight AIE performance of TPEQH, its fluorescence spectra in either THF/H_2O mixture or pure THF was investigated (Figure 3). The results demonstrated that TPEQH dissolved in THF emitted dim kelly fluorescence (Figure 3A). Moreover, when the water fraction (f_w) in the mixture solvent was adjusted from 10% to 70%, the fluorescence intensities of TPEQH kept almost constant but gradually red-shifted from 515 nm to 543 nm. Like all of other AIE fluorophores, the weak fluorescence of TPEQH in the dilute solution was attributed to the intramolecular free rotations of chemical bond. Additionally, with the increase of the solvent polarity by the enhanced water content, the emission of TPEQH (with donor-acceptor structure) was red-shifted.[38] However, when the f_w continuously increased to 80% and 95%, the fluorescence intensities of TPEQH exhibited obvious enhancement due to the aggregation of TPEQH and the restricted intramolecular free rotations, which made the pathway of radioactive-decay prior to nonradioactive-decay for the photoexcited fluorophore to relax. To further understand the AIE performance of TPEQH, its emissive spectra under different concentrations were studied with the excitation wavelength of 353 nm in the THF (Figure 3B). The results indicated that, in the dilute solution (1×10^{-7}, 1×10^{-6} and 1×10^{-5} M), the fluorescence performance of TPEQH showed low correlation to the concentrations. However, as the concentrations continued to increase (1×10^{-4}, 1×10^{-3} and 1×10^{-2} M), the fluorescence intensity increased significantly, reflecting the excellent AIE performance of TPEQH

Journal Pre-proofs

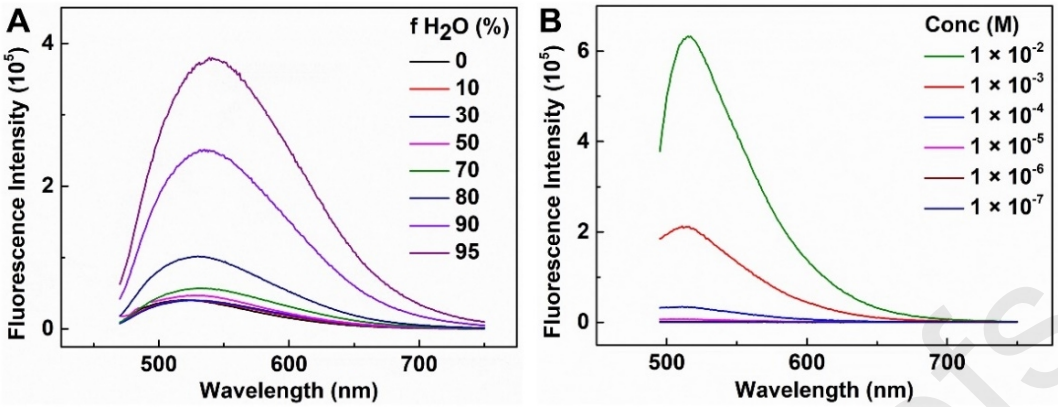

Figure 3. The AIE property of TPEQHA. (A) The emission spectra of TPEQH in the mixture of THF and deionized water. (B) The emission spectra of TPEQH with different concentrations in pure THF.

3.3 Theoretical Investigations. Quantum chemical calculations about the TPEOH optical behaviors when responding to the intracellular ALP were then conducted using B3LYP/6-31G* method via Gaussian 09 program. The frontier molecular orbitals (including HOMO and LUMO) and the optimized structures of TPEQH molecule were demonstrated in Figure 4. The results indicated that the highest occupied molecular orbital (HOMO) was localized on the TPE unit. The quinoxalinone structure made less contribution to the HOMO. However, the lowest unoccupied molecular orbital (LUMO) was mainly localized on the quinoxalinone structure, but was also influenced by the phenyl ring of the TPE. Additionally, the HOMO-1 was localized on the whole molecule while LUMO+1 was TPE centered. The quinoxalinone structure of TPEQH had less contribution to the LUMO+1. The localized frontier molecular orbitals of TPEQH showed that, when encountering photoexcitation, the charge of the TPEQH molecule would redistribute. Meanwhile, the absorbed energy of TPE could be consumed via the free rotation of chemical bonds around the central double bond. As a result, when rotation was restricted, the fluorescence properties of TPEQH appeared.

Journal Pre-proofs

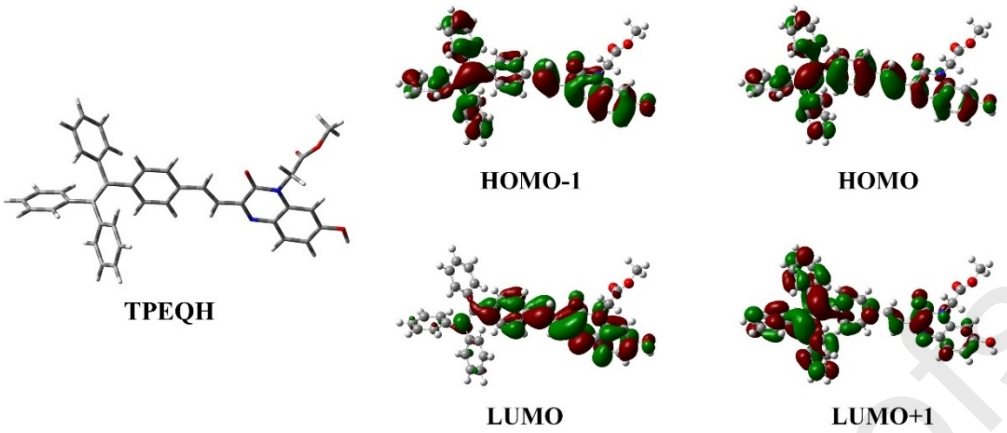

Figure 4. Optimized structures and frontier molecular orbitals for TPEQH. Calculations were carried out by density functional theory calculations at the B3LYP/6-31G* level.

3.4 The Fluorescence Response of TPEQHA to ALP in Solutions. In order to investigate the fluorescence response behavior of TPEQHA, the interaction between TPEQHA and different concentrations of ALP was investigated. Without ALP response, the water soluble TPEQHA showed dim fluorescence. When TPEQHA was cultured with ALP at different concentrations for 20 min, the phosphate group of TPEQHA was hydrolyzed and converted to TPEQH, which was hydrophobic and self-aggregated in solution. Thus, the fluorescence in the solution was gradually enhanced over the increase of the ALP concentration (0-180 U/L, shown in Figure 5A). Figure 5B has shown the fluorescence intensity change with the change of ALP concentration. After further analysis of the experimental results (Figure 5C), an approximate first-order linear correlation from 0 to 100 U/L (R^2 = 0.9985) was described, thus the intracellular detection limit of ALP of (1.77 U/L, 3σ/slope rule) was deduced[22]. Namely, the response fluorescence of TPEQH not only demonstrated its specificity to the ALP, but also manifested that TPEQHA was able to recognize ALP with high efficiency.

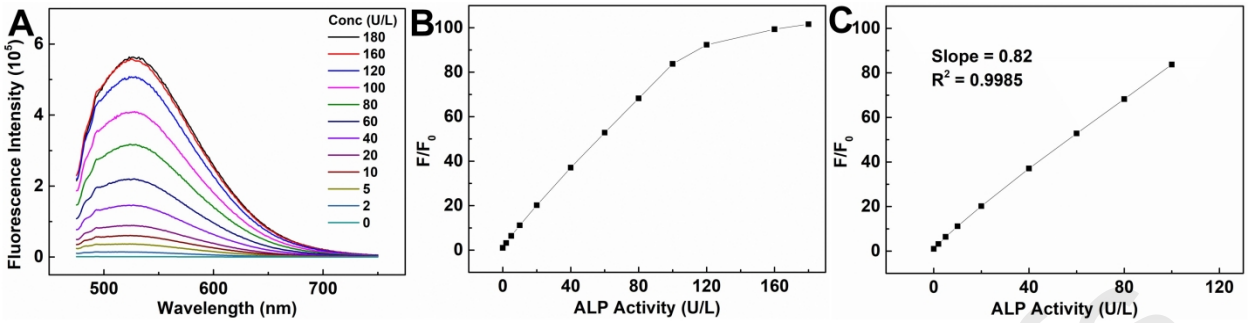

Figure 5. The response of TPEQHA to ALP. (A) The fluorescence intensity changes of TPEQHA upon the different concentrations of ALP (0-10 U/L). (B) The correlation of TPEQHA with the different concentrations of ALP. (C) The approximate first-order linear correlation of TPEQHA with ALP.

3.5 In Vitro Cytotoxicity and Cellular Uptake investigation. Since TPEQH was utilized for ALP imaging in the living cells, a standard MTT assay on the L929 and HeLa cells was conducted to estimated the potential cytotoxicity of TPEQH. HeLa cell overexpressed ALP was considered as the model target cell, and L929 with normal ALP expression was used as the negative control.[35,36] These two cells samples were co-incubated with TPEQH (20 μM) for 48 h. As the results demonstrated in Figure 6, the cell viability of both two cell samples remained more than 80%, indicating that TPEQH was low cytotoxicity and qualified for living cell imaging.

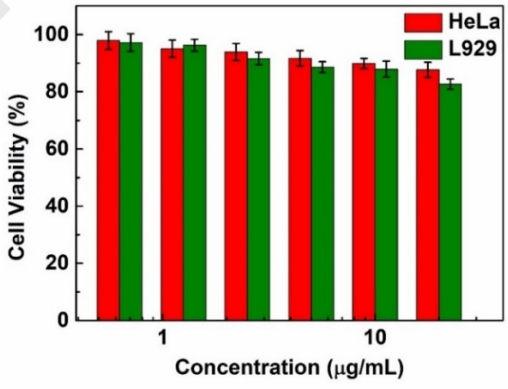

Figure 6. Cell viability of HeLa and L929 cells treated for 48 h with different concentrations of TPEQH (n = 5).

3.6 Intracellular Imaging of TPEQH. Having demonstrated its successful ability to respond to ALP in solution, the ALP imaging by TPEQHA was then performed in living cells (HeLa and L929 cell). Then, the response behavior between TPEQHA and ALP in these two kinds of cell were further analyzed using a flow cytometry and CLSM.

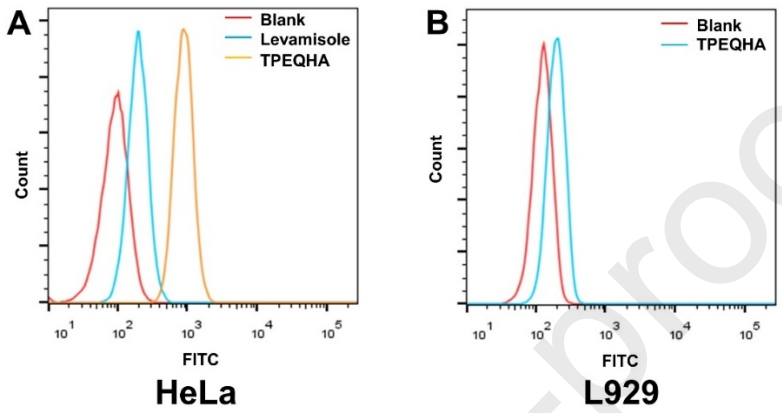

Figure 7. Flow cytometry analysis in Hela and L929 cells after a 1 h treatment with TPEQHA. (A) Flow cytometry analysis of TPEQH in Hela cell. (B) Flow cytometry analysis of TPEQH in L929 cell.

Firstly, HeLa and L929 cells were treated with TPEQHA for 1 h. Another group of HeLa cells was pretreated with levamisole hydrochloride for 30 minutes and then incubated with fluorescent probe for 1 hour. The results were measured by flow cytometry (Figure 7). Strong fluorescence could be detected while in HeLa cells, while the fluorescence was weak in both L929 cells and HeLa cells treated with levamisole hydrochloride. These results demonstrated that the phosphate group of TPEQHA was hydrolyzed by ALP in HeLa cells and TPEQHA was converted to hydrophobic TPEQH. TPEQH self-aggregated in the cells and emitted bright fluorescence. In two other kinds of cells, ALP expression was either low or inhibited, which was unable to hydrolyze phosphate. As a result, the fluorescence was weak. Namely, ALP expression could be efficiently

Journal Pre-proofs

distinguished by TPEQHA in living cells, making tumor cells and normal cells be successfully differentiated.

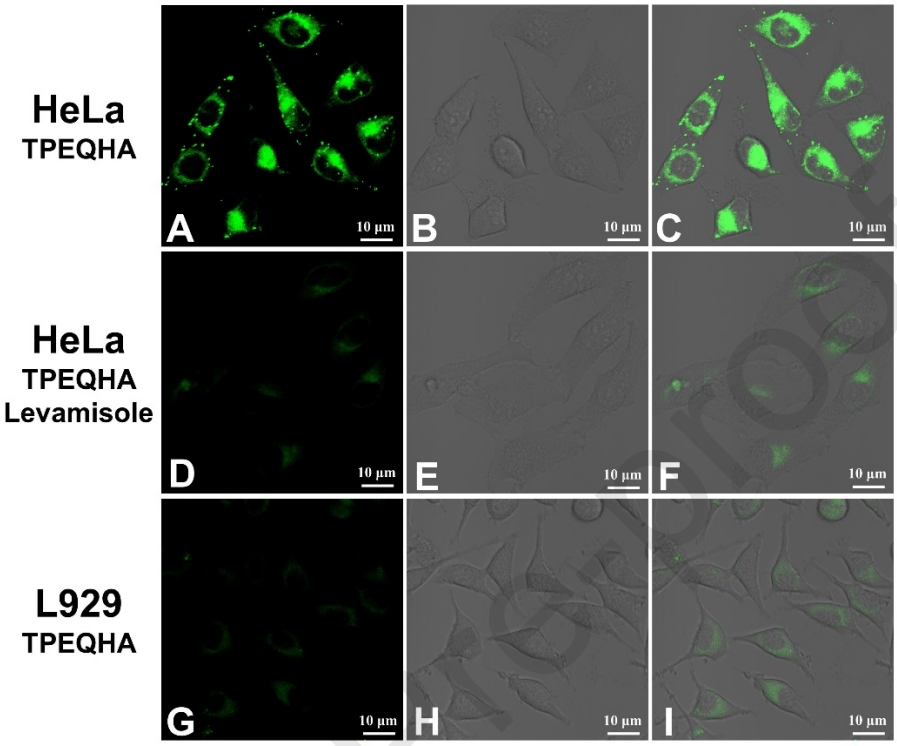

Figure 8. CLSM images of HeLa and L929 cells after treating with TPEQHA for 1 h. (A, B, C) The fluorescence of TPEQH is displayed as green dots on the cytomembrance of HeLa cell by exciting at a 488 nm laser. (D, E, F) In HeLa cell treated with levamisole, weak fluorescence of TPEQH is observed. (G, H, I) Weak fluorescence of TPEQH is observed in L929 cell.

To obtain more intuitive fluorescence images after ALP response, the cells were observed with CLSM. HeLa cells, L929 cells and HeLa cells treated with levamisole hydrochloride were incubated with TPEQHA for 1 h in the confocal dishes, followed by the direct observation with CLSM (Figure 8). The results shown in Figure 8A, B and C demonstrated that strong green fluorescence in HeLa cells was observed. In contrast, weak fluorescence was observed in L929 cells and HeLa cells treated with levamisole hydrochloride, which were consistent with the results of flow cytometry.

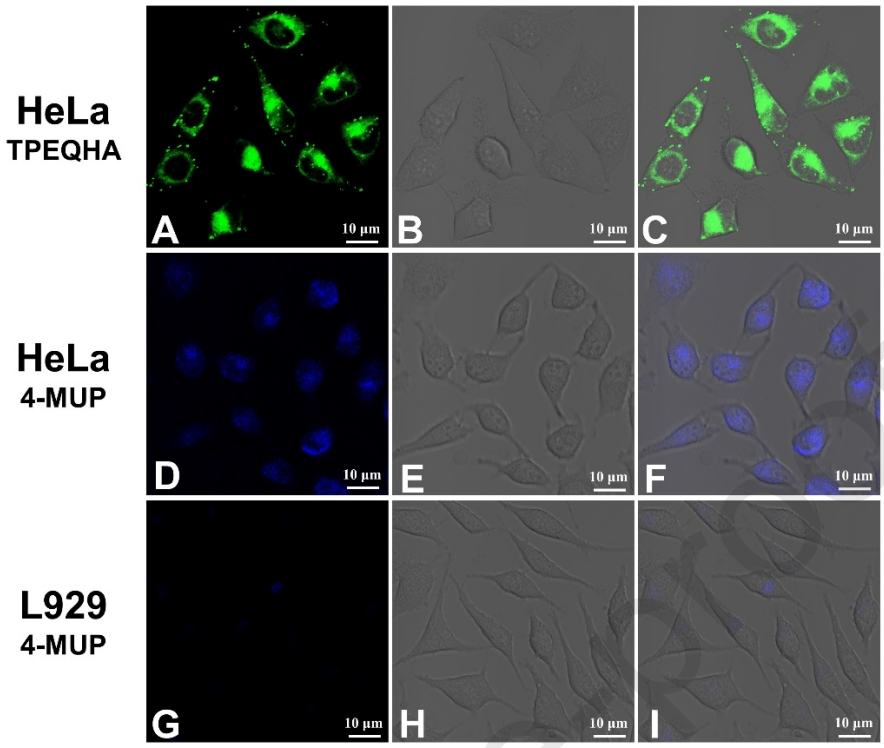

Figure 9. CLSM images of HeLa cell after treating with TPEQHA or 4-MUP for 1 h. The fluorescence of TPEQH is displayed as green dots on the cytomembrane of HeLa cells by exciting at a 488 nm laser (A, B, C). Blue fluorescence of 4-MUP diffused in HeLa cell (D, E, F). Weak blue fluorescence of 4-MUP is observed in L929 cells (G, H, I).

Finally, to determine the in-situ imaging effect of ALP in cells with TPEQHA, a commercially available probe 4-MUP was selected as a control, in which 4-MUP was used as an ACQ fluorescence probe for ALP imaging in living cells. In HeLa cells treated with 4-MUP, blue fluorescence could be detected, but diffused throughout the cell and resulted in less contrasting, thereby gradually losing signal intensity (9D, E and F). However, when replaced with TPEQHA, green fluorescence gathered together in HeLa cells and was presented in the form of bright fluorescent dots, reflecting that the signal of TPEQH remained stable *in situ* (9A, B and C). These results further illustrated that the solid TPEQH dye used for in-situ ALP imaging in living cells had enhanced resolution and accuracy.

4. CONCLUSIONS

In conclusion, we have developed an AIE fluorescence probe (TPEQH) and exploited its application as an enzyme-response AIE probe to detect ALP in situ in cancer cells. When dissolved in the solvent, TPEQH showed high insolubility and splendid AIE characteristics. Its intense fluorescence in the solid state and wide range of excitation wavelength made it particularly suitable for in-situ imaging. *In vitro*, TPEQHA could image endogenous ALP with a large signal-to-background ratio in tumor cells. Compared with the ACQ fluorescent probe 4-MUP, TPEQHA could image ALP in situ and improve the contrast and accuracy of detection in living tumor cells. The experiment results show that we have successfully synthesized a new fluorophore with remarkable AIE property, and further deceloped an AIE fluorescence probe for in situ imaging ALP to improve contrast and accuracy of detection result. We considered that the new ALP-responsive probe had a great potential to be a powerful tool to reveal the function of ALP in various pathological processes.

ACKNOWLEDGMENTS

This work was financially supported by the National Basic Research Program (2015CB931801) and the National Natural Science Foundation of China (51473093, 21374062), the National Basic Research Program (2015CB931801), Shanghai Municipal Science and Technology Commission 2019 “Science and Technology Innovation Action Plan” Funded Project (19441905900)

Author Contribution

Journal Pre-proofs

Qinghua Guan and Xinmiao Lu contributed equally to this work and were considered as the co-first author.

Conflict of Interest

The authors declare no conflicts of interest.

REFERENCES

[1] Guo, Z.; Park, S.; Yoon. J.; et al. Recent Progress in the Development of Near-Infrared Fluorescent Probes for Bioimaging Applications. *Chem. Soc. Rev.* **2014,** *43,* 16-29.

[2] Sun, W.; Guo, S.; Hu, C.; et al. Recent Development of Chemosensors Based on Cyanine Platforms. *Chem. Rev.* **2016,** *116,* 7768-7817

[3] Xu, K.; Luan, D.; Wang, X.; et al. An Ultrasensitive Cyclization-Based Fluorescent Probe for Imaging Native HOBr in Live Cells and Zebrafish. *Ange. Chem. Int. Ed.* **2016,** *55,* 12751-12754.

[4] Boonacker, E.; Van, Noorden. C. J. F. Enzyme Cytochemical Techniques for Metabolic Mapping in Living Cells, with Special Reference to Proteolysis. *Histochem. Cytochem.* **2001,** *49,* 1473-1486

[5] Chen, X.; Lee, D.; Yu, S.; et al. In vivo Near-Infrared Imaging and Phototherapy of Tumors Using a Cathepsin B-Activated Fluorescent Probe. *Biomaterials.* **2017,** *122,* 130-140

[6] Shi, H.; Kwok, R. T. K.; Liu, J.; et al. Real-Time Monitoring of Cell Apoptosis and Drug Screening Using Fluorescent Light-Up Probe with Aggregation-Induced Emission Characteristics. *J. Am. Chem. Soc.* **2012,** *134,* 17972-17981.

Journal Pre-proofs

[7] Wu, X.; Li, L.; Shi, W.; et al. Near-Infrared Fluorescent Probe with New Recognition Moiety for Specific Detection of Tyrosinase Activity: Design, Synthesis, and Application in Living Cells and Zebrafish. *Ange. Chem. Int. Ed.* **2016,** *55,* 14728-14732.

[7] Gu, K.; Xu, Y.; Li, H.; et al. Real-Time Tracking and in vivo Visualization of β-Galactosidase Activity in Colorectal Tumor with a Ratiometric Near-Infrared Fluorescent Probe. *J. Am. Chem. Soc.* **2016,** *138,* 5334-5340

[9] Song, Z.; Kwok, R. T. K.; Zhao, E.; et al. A Ratiometric Fluorescent Probe Based on ESIPT and AIE Processes for Alkaline Phosphatase Activity Assay and Visualization in Living Cells. *ACS Appl. Mater. Interfaces.* **2014,** *6,* 17245-17254.

[10] Chen, X.; Zhou, Y.; Peng, X.; et al. Fluorescent and Colorimetric Probes for Detection of Thiols. *Chem. Soc. Rev.* **2010,** *39,* 2120-2135

[11] Li, X.; Gao, X.; Shi, W.; et al. Design Strategies for Water-Soluble Small Molecular Chromogenic and Fluorogenic Probes. *Chem. Rev.* **2014,** *114,* 590-659.

[12] Xu, Q.; Heo, C. H.; Kim, J. A.; et al. A Selective Imidazoline-2-thione-bearing Two-Photon Fluorescent Probe for Hypochlorous Acid in Mitochondria. *Anal. Chem.* **2016,** *88,* 6615-6620

[13] Leung, C. W. T.; Hong, Y.; Chen, S.; et al. A Photostable AIE Luminogen for Specific Mitochondrial Imaging and Tracking. *J. Am. Chem. Soc.* **2013,** *135,* 62-65.

[14] Zhou, J.; Shi, W.; Li, L.; et al. Detection of Misdistribution of Tyrosinase from Melanosomes to Lysosomes and its Upregulation Under Psoralen/Ultraviolet a with a Melanosome-Targeting Tyrosinase Fluorescent Probe. *Anal. Chem.* **2016,** *88,* 4557-4564.

[15] Birks, J. B. Photophysics of Aromatic Molecules. Wiley: New York, **1970**.

[16] Hu, R.; Leung, N. L.; Tang, B. Z. AIE Macromolecules: Syntheses, Structures and Functionalities. *Chem. Soc. Rev.* **2014,** *43,* 4494-4562.

Journal Pre-proofs

[17] Ding, D.; Li, K.; Liu, B.; et al. Probes Based on AIE Fluorogens. *ACS. Chem. Res.* **2013,** *46,* 2441-2453.

[18] Zhou, L.; Zhang, X.; Lv, Y.; et al. Localizable and Photoactivatable Fluorophore for Spatiotemporal Two-Photon Bioimaging. *Anal. Chem.* **2015,** *87,* 5626-5631.

[19] Zhang, X.; Waibel, M.; Hasserodt, J. An Autoimmolative Spacer Allows First - Time Incorporation of a Unique Solid-State Fluorophore into a Detection Probe for Acyl Hydrolases. *Chem. Eur. J.* **2010,** *16,* 792-795.

[20] Thorn-Seshold, O.; Vargas-Sanchez, M.; McKeon, S.; et al. A Robust, High-Sensitivity Stealth Probe for Peptidases. *Chem. Commun.* **2012,** *48,* 6253-6255.

[21] SuáLim, C.; MyungáKim, H. A Two-Photon Fluorescent Probe for Specific Detection of Hydrogen Sulfide Based on a Familiar ESIPT Fluorophore Bearing AIE Characteristics. *Chem. Commun.* **2017,** *53,* 4791-4794.

[22] Coleman, J. E. Structure and Mechanism of Alkaline Phosphatase. *Annu. Rev. Biophys. Biomol. Struct.* **1992,** *21,* 441-483.

[23] Shi, Y. Serine/Threonine Phosphatases: Mechanism through Structure. *Cell.* **2009,** *139,* 468-484.

[24] Herz, F. Alkaline Phosphatase Isozymes in Cultured Human Cancer Cells. *Experientia.* **1985,** *41,* 1357-1361.

[25] Tonks, N. K. Protein Tyrosine Phosphatases: from Genes, to Function, to Disease. *Nat. Rev. Mol. Cell Biol.* **2006,** *7,* 833.

Journal Pre-proofs

[26] Wolf, P. L. Clinical Significance of Serum High - Molecular - Mass Alkaline Phosphatase, Alkaline Phosphatase-Lipoprotein - X Complex, and Intestinal Variant Alkaline Phosphatase. *J. Clin. Lab. Anal.* **1994,** *8,* 172-176.

[27] Lange, P. H.; Millan, J. L.; Stigbrand, T.; et al. Placental Alkaline Phosphatase as a Tumor Marker for Seminoma. *Cancer Res.* **1982,** *42,* 3244-3247.

[28] Fraser, W. D. Paget's Disease of Bone. *Curr. Opin. Orthop.* **1997,** *9,* 347-354.

[29] Frisch, M. J.; Trucks, G. W.; Schlegel, H. B.; et al. Gaussian 09, revision D. 01; Gaussian, Inc. Wallingford CT, **2013.**

[30] Vosko, S.; Wilk, L.; Nusair, M. Accurate Spin-Dependent Electron Liquid Correlation Energies for Local Spin Density Calculations: A Critical Analysis. *Can. J. Phys.* **1980,** *58,* 1200-1211.

[31] Becke, A. D. Density-Functional Thermochemistry. V. Systematic Optimization of Exchange-Correlation Functionals. *J. Chem. Phys.* **1997,** *107,* 8554-8560.

[32] Kohn, W.; Becke, A. D.; Parr, R. G. Density Functional Theory of Electronic Structure. *J. Phys. Chem.* **1996,** *100,* 12974-12980.

[33] Song, Z.; Kwok, R. T. K.; Zhao, E.; et al. A Ratiometric Fluorescent Probe Based on ESIPT and AIE Processes for Alkaline Phosphatase Activity Assay and Visualization in Living Cells. *ACS Appl. Mater. Interfaces.* **2014,** *6,* 17245-17254.

[34] Hou, X.; Yu, Q.; Zeng, F.; et al. A Ratiometric Fluorescent Probe for in vivo Tracking of Alkaline Phosphatase Level Variation Resulting from Drug-Induced Organ Damage. *J. Mater. Chem. B.* **2015,** *3,* 1042-1048.

Journal Pre-proofs

[35] Liu, H.; Lv, Z.; Ding, K.; et al. Incorporation of Tyrosine Phosphate into Tetraphenylethylene Affords an Amphiphilic Molecule for Alkaline Phosphatase Detection, Hydrogelation and Calcium Mineralization. *J. Mater. Chem. B*. **2013,** *1,* 5550-5556.

[36] Lin, M.; Huang, J.; Zeng, F.; et al. A Fluorescent Probe with Aggregation-Induced Emission for Detecting Alkaline Phosphatase and Cell Imaging. *Chem. Asian. J.* **2019,** *14,* 802-808.

Figure caption

Figure 1: Synthesis of TPEQH and TPEQHA.

Figure 2: Optical properties of TPEQH. (A) Fluorescent excitation and emission spectra of TPEQ solid. (B) The UV-vis absorption spectrum of TPEQ in pure THF (1×10^{-5} M). (C) The UV-Vis absorption spectrum of TPEQ (1×10^{-5} M) in different solution (THF, Acetone, DMSO, MeOH). (D) The fluorescent emission spectra of TPEQ (1×10^{-3} M) in different solution (THF, Acetone, DMSO, MeOH) with 475 nm laser.

Figure 3: The AIE property of TPEQHA. (A) The emission spectra of TPEQH in the mixture of THF and deionized water. (B) The emission spectra of TPEQH with different concentrations in pure THF.

Figure 4: Optimized structures and frontier molecular orbitals for TPEQH. Calculations were carried out by density functional theory calculations at the B3LYP/6-31G* level.

Figure 5: The response of TPEQHA to ALP. (A) The fluorescence intensity changes of TPEQHA upon the different concentrations of ALP (0-10 U/L). (B) The correlation of TPEQHA with the different concentrations of ALP. (C) The approximate first-order linear correlation of TPEQHA with ALP.

Journal Pre-proofs

Figure 6: Cell viability of HeLa and L929 cells treated for 48 h with different concentrations of TPEQH (n = 5).

Figure 7: Flow cytometry analysis in HepG2 and L929 cells after a 1 h treatment with TPEQHA. (A) Flow cytometry analysis of TPEQH in HepG2 cell. (B) Flow cytometry analysis of TPEQH in L929 cell.

Figure 8: CLSM images of HeLa and L929 cells after treating with TPEQHA for 1 h. (A, B, C) The fluorescence of TPEQH is displayed as green dots on the cytomembrance of HeLa cell by exciting at a 488 nm laser. (D, E, F) In HeLa cell treated with levamisole, weak fluorescence of TPEQH is observed. (G, H, I) Weak fluorescence of TPEQH is observed in L929 cell.

Figure 9: CLSM images of HeLa cell after treating with TPEQHA or 4-MUP for 1 h. (A, B, C) The fluorescence of TPEQH is displayed as green dots on the cytomembrance of HeLa cells by exciting at a 488 nm laser. (D, E, F) Blue fluorescence of 4-MUP diffused in HeLa cell. (G, H, I) Weak blue fluorescence of 4-MUP is observed in L929 cells.

Journal Pre-proofs

Graphical Abstract

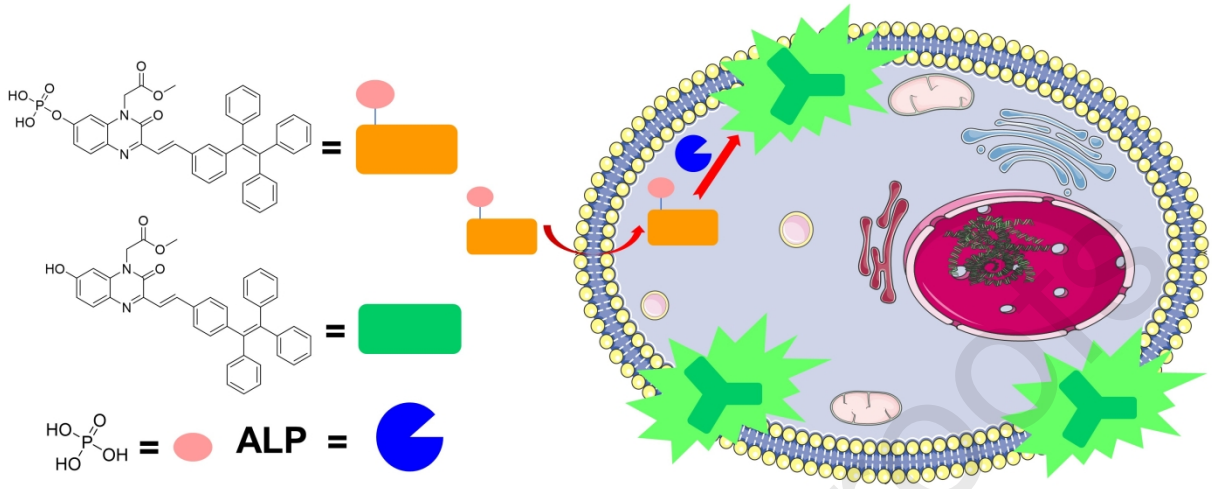

Journal Pre-proofs

Supporting Information

In Situ Localization of Alkaline Phosphatase Activity in Tumor Cells by an Aggregation-Induced Emission Fluorophore-Based Probes

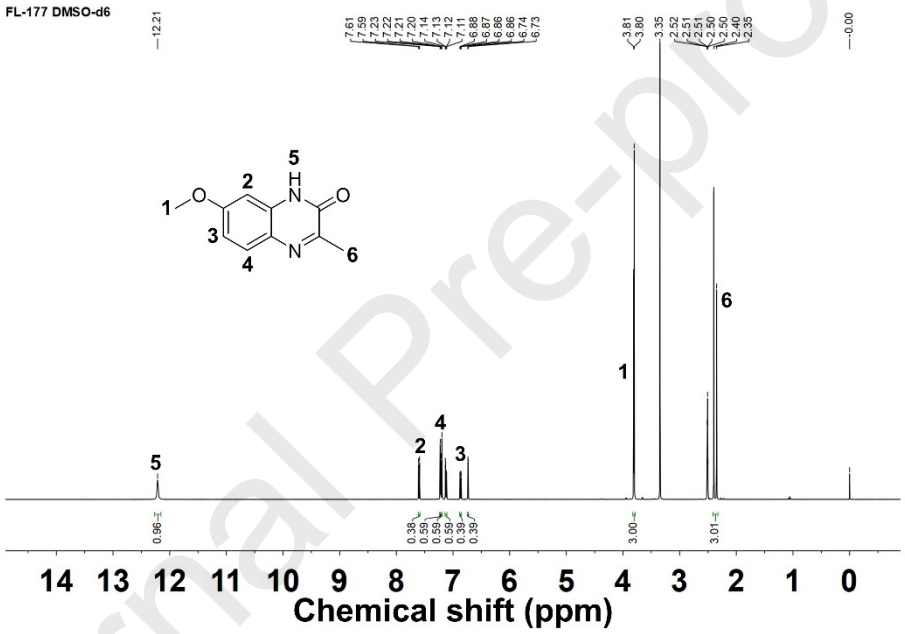

Journal Pre-proofs

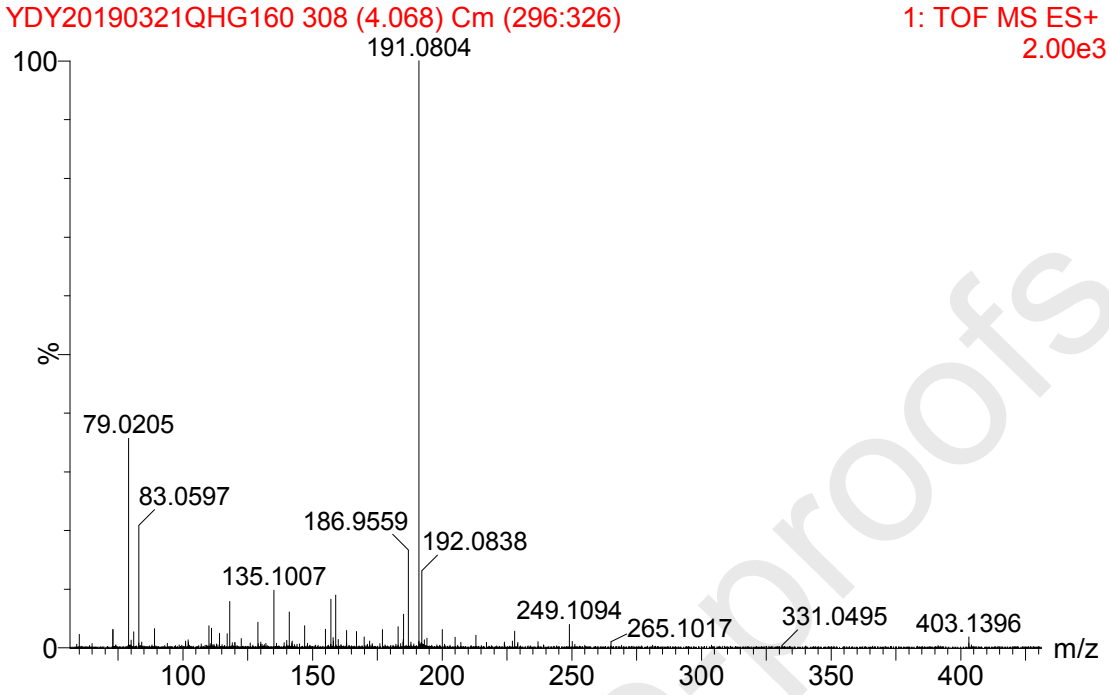

Figure S1. The ^{1}H NMR (up) and MS (down) spectra of compound (1). ^{1}H NMR (400 MHz, DMSO-d6, δ): 12.21 (s, 1H), 7.61, 7.21 (1H), 7.23, 6.74 (1H), 7.14, 6.88 (1H), 3.81 (3H), 2.4 (2H).

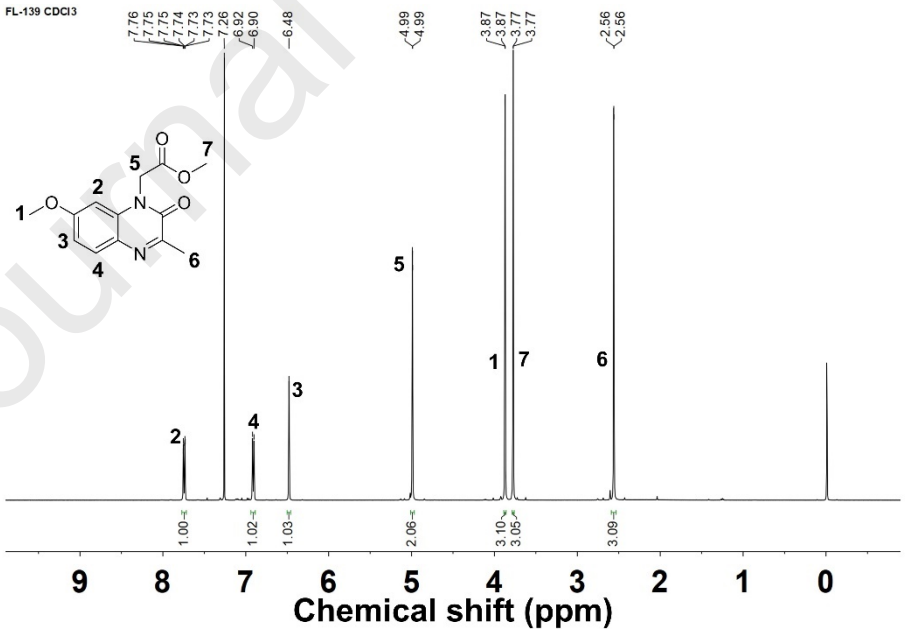

Journal Pre-proofs

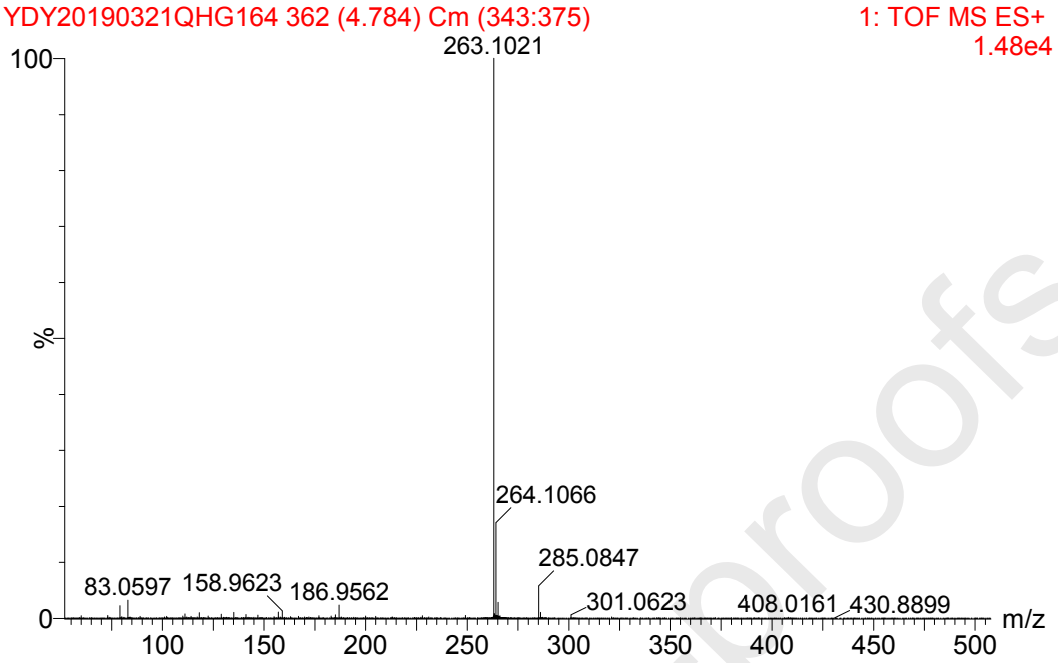

Figure S2. The ^{1}H NMR (up) and MS (down) spectra of compound (2). ^{1}H NMR (400 MHz, $CDCl_3$, δ): 7.76 (d, 1H), 6.92 (d, 1H), 6.48 (s, 1H), 4.99 (s, 2H), 3.87 (s, 3H), 3.77 (s, 3H), 2.56 (s, 3H).

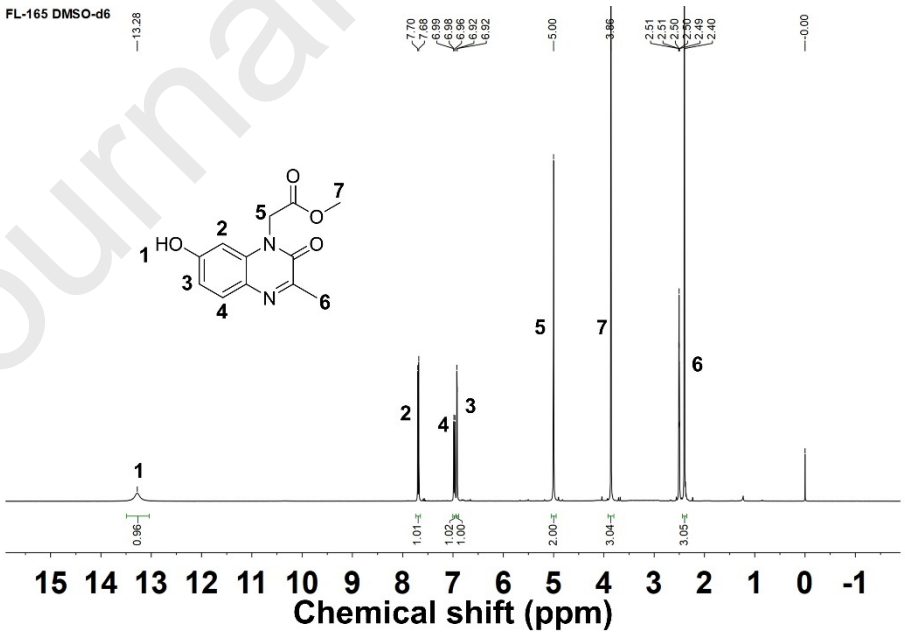

Journal Pre-proofs

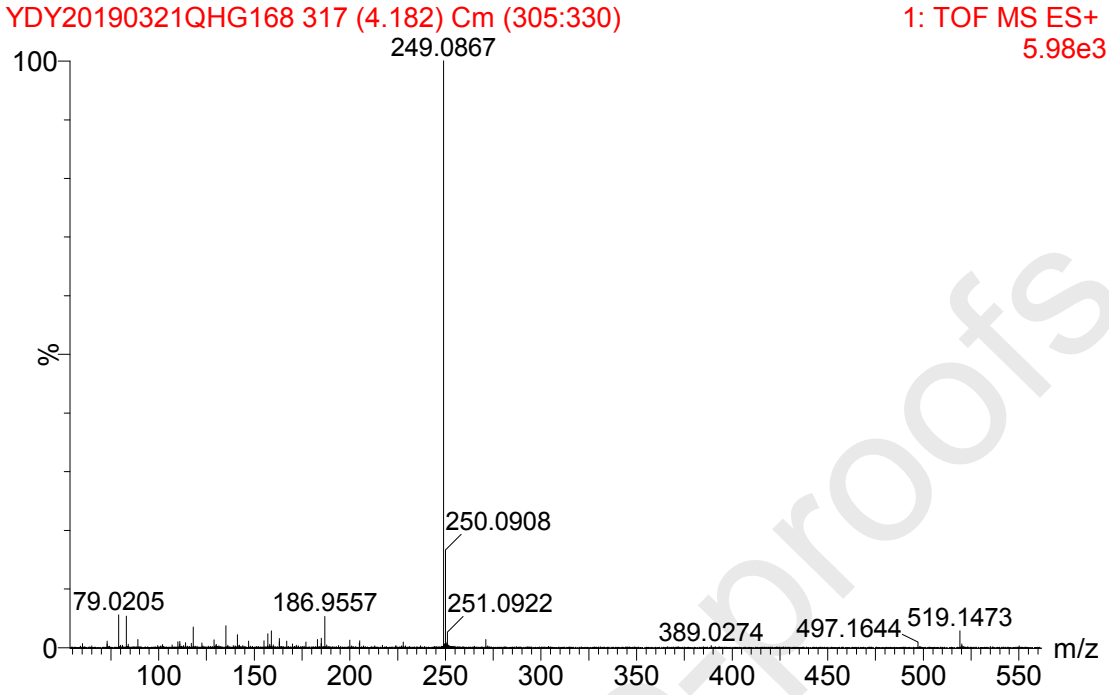

Figure S3. The ^{1}H NMR (up), ^{13}C NMR (middle) and MS (down) spectra of compound (3). ^{1}H NMR (400 MHz, DMSO-d6, δ): 13.82 (s, 1H), 7.70 (d, 1H), 6.99 (d, 1H), 6.92 (s, 1H), 5.00 (s, 2H), 3.86 (s, 3H), 2.40 (s, 3H).

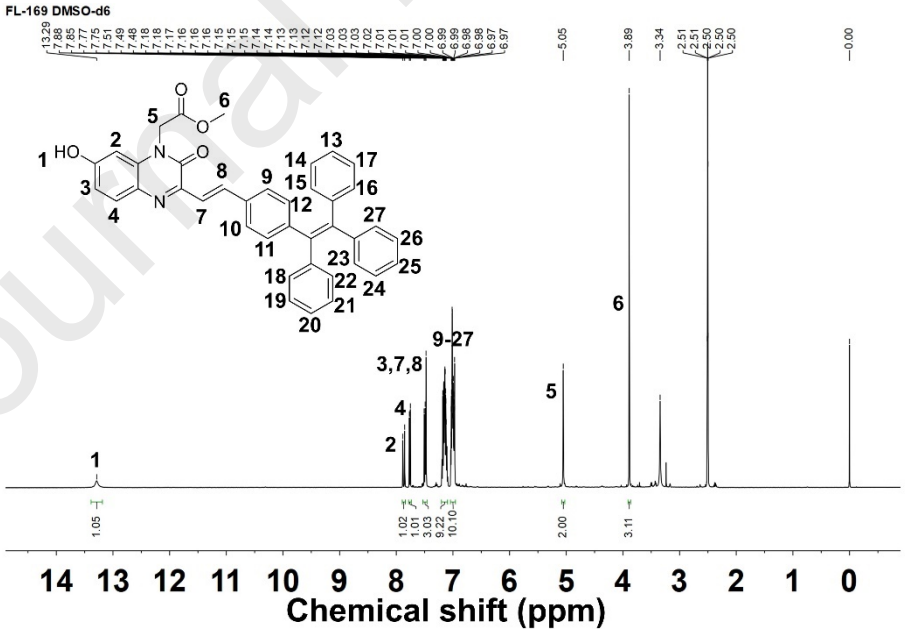

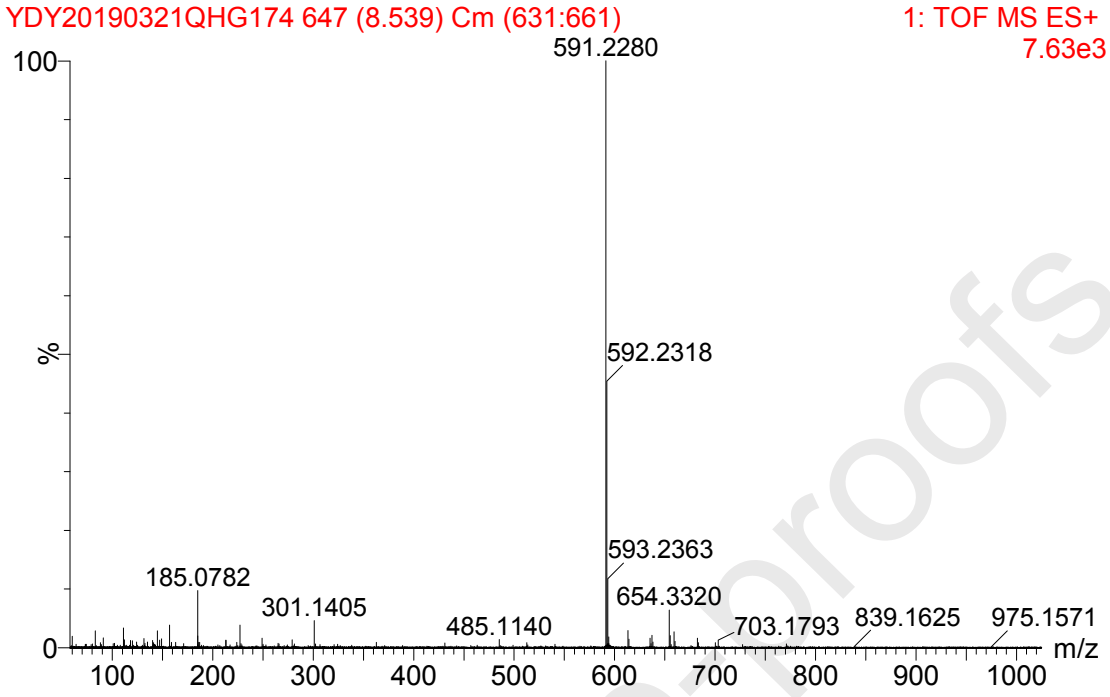

Figure S4. The ^{1}H NMR (up) and MS (down) spectra of compound (4). ^{1}H NMR (400 MHz, DMSO-d6, δ): 13.29 (s, 1H), 7.88 (d, 1H), 7.77 (d, 1H), 7.51 (3H), 7.18 (9H), 7.03 (10H), 5.05 (s, 2H), 3.89 (s, 3H).

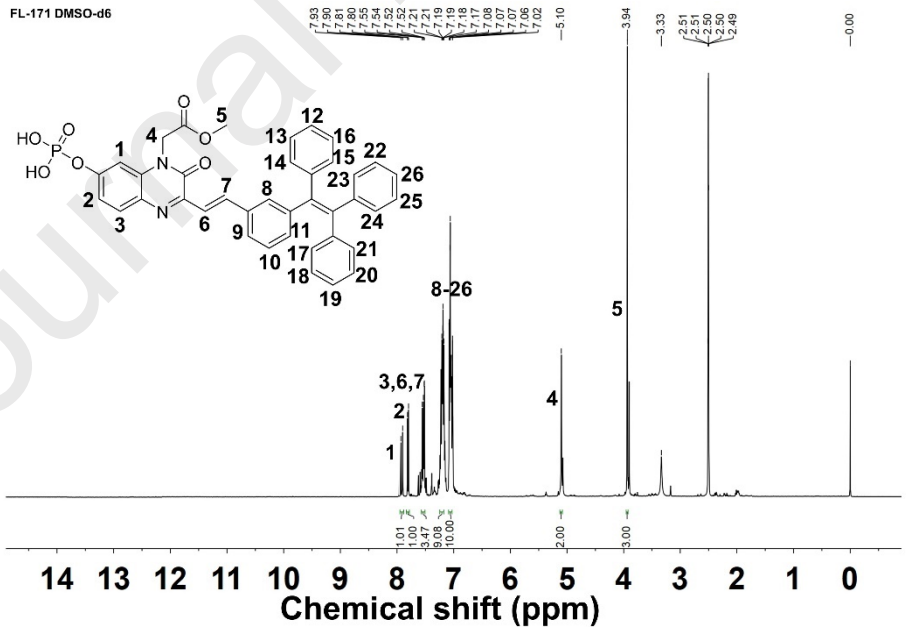

Journal Pre-proofs

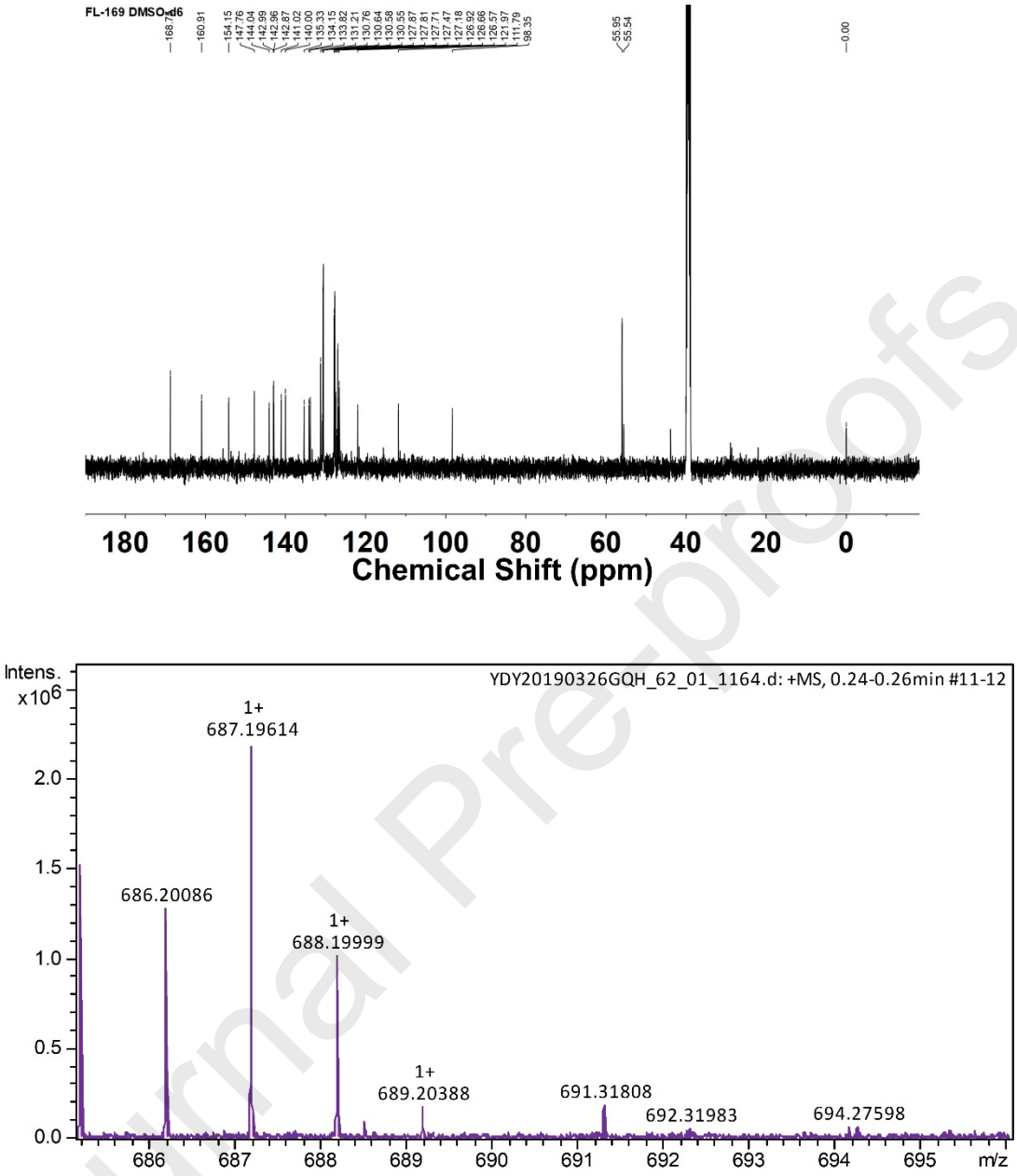

Figure S5. The ^{1}H NMR (up) and MS (down) spectra of compound (5). ^{1}H NMR (400 MHz, DMSO-d6, δ): 7.93 (d, 1H), 7.81 (d, 1H), 7.54 (3H), 7.21 (9H), 7.08 (10H), 5.10 (s, 2H), 3.94 (s, 3H). ^{13}C NMR (100 MHz, DMSO-d6, δ): 168.7, 160.91, 154.15, 147.76, 144.04, 142.99, 142.96, 142.87, 141.02, 140.00, 135.33, 134.15, 133.82, 131.21, 130.76, 130.64, 130.58, 130.55, 127.87, 127.81, 127.71, 127.47, 127.18, 126.92, 126.66, 126.57, 121.97, 111.79, 98.35, 55.95, 55.54.

Graphical abstract

Journal Pre-proofs

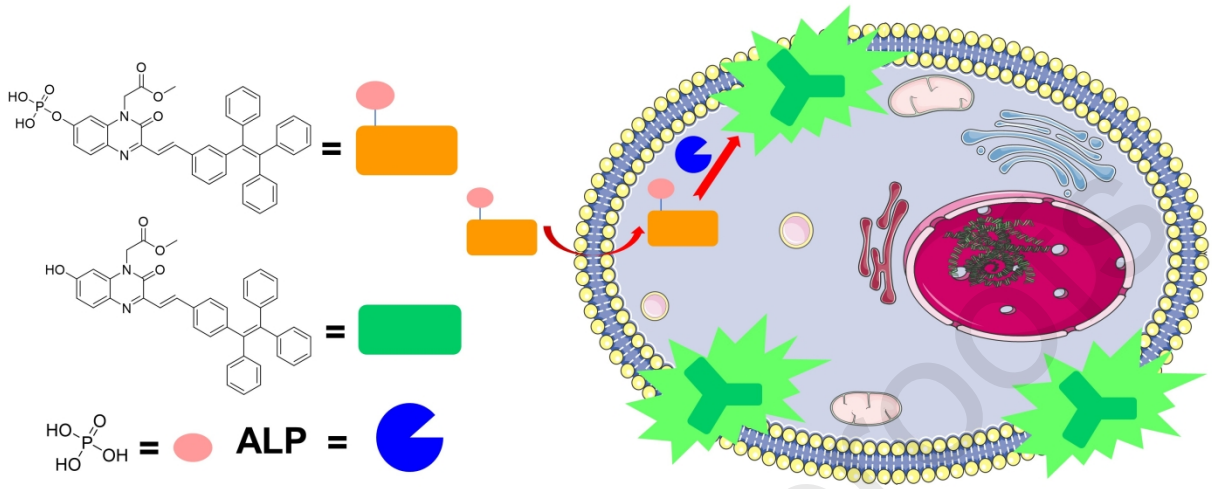

Journal Pre-proofs

Conflict of interest

The authors declared that they have no conflicts of interest to this work.

Journal Pre-proofs